PHYSICAL REVIEW B VOLUME 40, NUMBER 7 1 SEPTEMBER 1989

Finite-size effects in continuum percolation

A.-M. S. Tremblay
Département de Physique et Centre de Recherche en Physique du Solide, Université de Sherbrooke, Sherbrooke, Québec, Canada J1K 2R1

J. Machta
Department of Physics and Astronomy, University of Massachusetts, Amherst, Massachusetts 01003
(Received 13 February 1989)

Corrections to scaling in percolation networks with a broad distribution of electrical resistances are studied analytically and numerically. Field-theoretic methods and a nodes-links-blobs approach are employed to calculate corrections to scaling. Two numerical methods are introduced to test the predicted corrections to scaling and to minimize finite-size effects. One is a parameterless numerical renormalization-group procedure and the other involves tuning, within the same universality class, the initial distribution describing the electrical resistance of the bonds. Finite-size effects are shown to be the source of the disagreement between past numerical work and theoretical predictions.

I. INTRODUCTION

In recent years there has been considerable interest in percolation networks in which the transport properties of the bonds in the network are chosen from a distribution with a power-law tail. The reason for this interest is twofold. Firstly, the dynamical exponents in this system depend continuously upon the power law characterizing the distribution so providing a nontrivial example where the microscopic probability distribution determines the universality class. Secondly, percolation networks with a broad distribution of bond strengths are closely related to continuum percolation[1,2] and thus to practical questions such as the conductivity of metal-insulator composites. Experiments have been carried out on metal-insulator composites[3] and on macroscopic realizations of the "Swiss cheese" model.[4,5] There are also a number of experiments on the related problem of current noise in percolating systems where continuum corrections are very important and appear in most experimental situations.[6]

Since the work of Kogut and Straley,[7] it has been known that dynamical exponents are modified by a broad distribution of bond strengths, although there has been disagreement in the literature[1,8–12] concerning the correct expression for the exponents. The disagreement among theoretical approaches was largely resolved by recent work[13,14] showing that the field-theoretic analysis[11] leads to the same prediction as the nodes-links-blobs analysis,[9,10] namely, that the conductivity exponent t, changes from its lattice value to the continuum percolation value at a critical value of the parameter, α, describing the tail of the broad distribution of bond strengths. Numerical simulations[11,15–19] on the other hand, have yielded conductivity exponents whose behavior as a function of α differs qualitatively from the field-theory and nodes-links-blobs predictions.

According to the theory, the only feature of the distribution of bond strengths which is relevant to the asymptotic transport properties is the characteristic exponent describing the tail of the distribution. However, other irrelevant features of the distribution may lead to important corrections to scaling. In the present paper we develop a theory of the corrections to scaling arising from the initial distribution of bond strengths and we test this theory by numerical simulations. These simulations allow us, in one case, to change the initial condition on the irrelevant variable to decrease its influence, and in the other case, to go to effectively much larger system sizes. Detailed numerical procedures for extracting the leading exponent and the corrections to scaling from finite-size data have been developed.[20] Here, the particular origin of the corrections to scaling allows us to exhibit their influence through the above two methods.

As discussed by Privman and Fisher,[20] it is a general fact that the finite-size convergence of estimates for exponents is governed asymptotically by the leading irrelevant-variable scaling exponent. This irrelevant variable, which leads to corrections in scaling is, in the present problem, a dimensionless quantity describing the shape of the stable distribution of random resistors. As a function of the parameters describing the power-law tail, the lattice and continuum fixed points exchange stability. As we explain below, this leads to a very small correction to scaling exponent, hence to very slow convergence to the asymptotic limit. Similar slowly decaying transients are likely to be present in other disordered systems with broad distributions of bond strengths such as diluted magnets with power-law distribution of coupling strengths.[21]

In the remainder of this section we introduce the percolation model and review previous results. In Sec. II, corrections to scaling are calculated. Section III is devoted to the numerical methods and results. The paper closes with a discussion.

The model which we study is a random resistor network on a two-dimensional square lattice. We consider

bond percolation with a fraction, p, of finite resistors and a fraction, $1-p$, of open bonds. The finite resistors are independently chosen from a distribution having a power-law tail such that

$$\text{Prob}\{R>X\}\sim X^{-\alpha} \text{ as } X\to\infty \ . \tag{1.1}$$

Here R is any of the finite resistors of the network and $0<\alpha<1$ characterizes the tail of the distribution.[22] We shall have occasion to consider several distributions satisfying Eq. (1.1), the simplest having a pure power-law density with a minimum resistance of unity,

$$\text{Prob}\{R>x\}=\begin{cases}1, & 0<X<1\\ X^{-\alpha}, & X\geq 1\end{cases} . \tag{1.2}$$

Hitherto all of the numerical simulations have been carried out using this distribution.

For infinite systems near p_c the conductivity, σ, of the network is described by the conductivity exponent, t, according to

$$\sigma\sim(p-p_c)^t \ . \tag{1.3}$$

The accepted theoretical result,[13,14] first enunciated by Straley,[9] is that

$$t=\max\{t_0, t(\alpha)\} \ . \tag{1.4}$$

Here t_0 is the universal lattice value,

$$t_0=(d-2)\nu+\phi_0 \ , \tag{1.5}$$

with $\phi_0/\nu=0.98$ (Ref. 23) for $d=2$ and

$$t(\alpha)=(d-2)\nu+1/\alpha \ , \tag{1.6}$$

where ν is the correlation length exponent ($\nu=\frac{4}{3}$ for $d=2$). Note that there is a crossover from universal to nonuniversal behavior when $\alpha=\alpha_c=1/\phi_0$ where, for two-dimensional percolation, $\alpha_c=0.77$.

Numerical work has yielded values of t which exceed the theoretical prediction, Eq. (1.4). For example, at $\alpha=0.5$ the prediction is $t=2$ but the numerical results are $t=2.27\pm0.13$ (Ref. 16) using exact enumeration of random walks on clusters with about 10^4 sites and $t=2.20\pm0.06$ (Ref. 15) using sparse matrix inversion and finite-size scaling with lattice sizes up to 50×50. For $\alpha=\frac{2}{3}$, the numerical result is $t=1.84\pm0.05$,[15] whereas the theoretical prediction is $t=1.5$. Other numerical investigations,[7–19] in the range $0.4\leq\alpha\leq1$, have consistently yielded values of t which exceed the theoretical predictions except for the smallest α considered, $\alpha=0.4$, where the agreement is reasonable. In fact, there is a definite trend towards improved agreement as α decreases. Nevertheless, we must conclude that either the theory is wrong for all but the smallest α, or the numerical results do not represent asymptotic exponents. The authors of the numerical studies note that when their methods are applied to ordinary precolation they yield accurate values of the universal exponent, t_0, thus leading credence to the view that the theory is wrong. We shall argue, however, that the conventional distribution defined in Eq. (12) leads to significant deviations from the asymptotic exponents up to very large system sizes.

II. CORRECTIONS TO SCALING

A. Recursion relations

In Ref. 11 a field-theoretic ε expansion for the percolation problem with a broad distribution of resistances was developed. This approach is based upon obtaining renormalization group flows in a two-parameter space. Roughly speaking, this is the space of probability distributions for the resistance of a system of size L. These distributions are parametrized by the two leading terms of their Laplace transform

$$f(z)\sim1-vz^{\alpha}+wz+\cdots \ , \tag{2.1}$$

with

$$f(z)=\int e^{-zR}p(R)dR \ , \tag{2.2}$$

where $p(R)$ is the probability density for the resistance. The parameter v describes the amplitude of the power-law tail of the distribution and is non-negative. If v vanishes, $-w$ is the mean of the distribution and must be positive. Flow equations for w and v take the form

$$\frac{d\ln w}{d\ln L}=1/\nu-E(w,v) \ , \tag{2.3a}$$

and

$$\frac{d\ln v}{d\ln L}=1/\nu \ , \tag{2.3b}$$

where E is a function of w and v. As discussed in Refs. 13 and 14, these recursion relations are most easily studied working with $-w$, which has dimensions of resistance, and with the dimensionless variable $h=(-w)^{-\alpha}v$. The recursion relations may then be written in the form

$$\frac{d\ln(-w)}{d\ln L}=\phi_0/\nu+g(\alpha,h) \ , \tag{2.4a}$$

$$\frac{d\ln h}{d\ln L}=(1-\alpha\phi_0)/\nu-\alpha g(\alpha,h) \ , \tag{2.4b}$$

where $\phi_0=t_0-(d-2)\nu$ and $g(\alpha,0)=0$. The nodes-link-blobs approach of Ref. 10, which is discussed in more detail below, yields recursion relations with the same general structure as Eqs. (2.4).

Let us first consider the case of small h. Expanding the right-hand side of Eqs. (2.4) to linear order in h, one obtains

$$\frac{d\ln(-w)}{d\ln L}=\phi_0/\nu+C(\alpha)h \ , \tag{2.5a}$$

and

$$\frac{d\ln h}{d\ln L}-(1-\alpha\phi_0)/\nu-\alpha C(\alpha)h \ . \tag{2.5b}$$

Here $C(\alpha)$ is a constant depending on α.

These recursion relations have two nontrivial fixed points at $\{w,h\}=\{0,0\}$ and $\{0,h^*=(1-\alpha\phi_0)/\nu\alpha C(\alpha)\}$.

The fixed point at the origin corresponds to ordinary percolation and the corresponding distribution of resistances has no power-law tail. The two fixed points exchange stability at the crossover value, $\alpha=\alpha_c=1/\phi_0$. For $\alpha<\alpha_c$, the finite h^* fixed point is stable and leads to the α-dependent exponent given in Eq. (1.6).

The variable h characterizes the relative amplitude of the tail of the distribution. It plays the role of a dimensionless coupling constant. Finite-size effects come from the slow convergence of h to its fixed-point value. To understand this, first notice that w is the only variable which has dimensions of resistance. We assume that it determines the scaling of the typical resistance. Usual finite-size scaling arguments then lead one to identify a length scale dependent conductivity $\sigma(L)$ as

$$\sigma(L)=-L^{2-d}[w(l)]^{-1} . \tag{2.6}$$

The left-hand side of Eq. (2.5a) is then related to the effective exponent, $t_{\rm eff}$ at length scale L, since

$$t_{\rm eff}/\nu\equiv-\frac{d\ln\sigma}{d\ln L}=d-2+\frac{d\ln(-w)}{d\ln L} . \tag{2.7}$$

In order to obtain $t_{\rm eff}$ we integrate Eq. (2.5b) starting from the initial value, h_0. The solution, $h(L)$, is inserted into Eq. (2.5a) with the result,

$$t_{\rm eff}=(d-2)\nu+\phi_0\pm\frac{\theta}{\alpha}\left[\frac{1}{\Delta L^{\mp\theta/\nu}+1}\right] \tag{2.8}$$

with upper sign for $\alpha<\alpha_c$ and the lower sign for $\alpha>\alpha_c$ and where

$$\theta=|\alpha\phi_0-1| , \tag{2.9}$$

and

$$\Delta=(h^*/h_0)-1 . \tag{2.10}$$

The quantity, Δ, measures the deviation of the distribution from the α-dependent fixed point at

$$h=h^*=(1-\alpha\phi_0)/[\nu\alpha C(\alpha)] .$$

For $\alpha<\alpha_c$, h^* is the stable fixed point, while for $\alpha>\alpha_c$ it is the unstable one. At the crossover point, $\alpha\to\alpha_c$, where the α-dependent and lattice fixed points merge, the correction to scaling exponent, θ, vanishes and one finds instead logarithmic corrections to power-law behavior.

Equations (2.7) and (2.8) are consistent with the general result, Eq. (4) of Ref. 20, which, in terms of the variables of the present problem, may be rewritten (excluding the analog of the magnetic field variable for simplicity) as

$$-w=L^{\phi/\nu}Y_{-w}(g_pL^{1/\nu},g_hL^{y_3}) ,$$

where here $g_p=(p-p_c)=0$, g_h is the nonlinear scaling field for the leading irrelevant variable, y_3 is the corresponding exponent and Y_{-w} is a scaling function which is analytic at $g_p=0$ and $g_h=0$. Indeed, integrating Eqs. (2.7) and (2.8) we find that near the corresponding stable fixed point $\phi=\phi_0$, $g_h=1/\Delta$, $y_3=-\theta/\nu$, and $Y_{-w}=C_1(1+g_hL^{y_3})^{1/\alpha}$ in the case $\alpha>\alpha_c$, while $\phi=1/\alpha$, $g_h=\Delta$, $y_3=-\theta/\nu$, and

$$Y_{-w}=C_2(1+g_hL^{y_3})^{1/\alpha}$$

in the case $\alpha<\alpha_c$, with C_1 and C_2 nonuniversal constants. g_h has been defined so that in all cases, the stable fixed point is at $g_h=0$.

From Eqs. (2.5) then, one has found that $-\theta/\nu$ as defined by Eq. (2.9) is the leading irrelevant exponent. Linearizing these equations around the *unstable* fixed point, we also find that, in both cases ($\alpha<\alpha_c$ and $\alpha>\alpha_c$), $+\theta/\nu$ is the crossover exponent that describes how h flows *away* from the unstable fixed point. This coincidence is valid only in the limit where both the stable and unstable fixed points are close to one another, that is in the vicinity of $\alpha=\alpha_c$. In that sense, however, the smallness of the irrelevant exponent, which in turn leads to the large corrections to scaling, is due to the fact that for a sizable range of values of α, the two fixed points which exchange stability at $\alpha=\alpha_c$ are close to each other. More generally, when $\alpha\ll\alpha_c$, the crossover exponent around the stable fixed point at $h=0$ is still given by Eq. (2.5). However, at the stable fixed point, h^* becomes quite large and to find the leading irrelevant exponent around this fixed point, it is preferable to go beyond Eq. (2.5) and to expand (2.4) around the fixed point at h^*. One obtains, with $\tilde h\equiv h-h^*$,

$$\frac{\partial\ln(-w)}{\partial\ln L}=\frac{1}{\nu\alpha}+\frac{\partial g}{\partial h^*}\tilde h , \tag{2.11a}$$

$$\frac{\partial\ln\tilde h}{\partial\ln L}=-\alpha\frac{\partial g}{\partial h^*}h^*-\left[\alpha\frac{\partial g}{\partial h^*}+\frac{\alpha}{2}\frac{\partial^2 g}{\partial h^{*2}}h^*\right]\tilde h$$

$$\equiv-\frac{\theta}{\nu}-B(\alpha)\tilde h , \tag{2.11b}$$

where $\theta/\nu\equiv(\partial g/\partial h^*)h^*$ and, if we define ϕ by $\phi=(1-\theta)/\alpha$, now ϕ is a function of α. Proceeding as before, we obtain

$$t_{\rm eff}=(d-2)\nu+\frac{1}{\alpha}+\frac{\theta/\alpha}{\frac{h^*}{\tilde h_0}\left[1+\frac{B(\alpha)}{\theta/\nu}\tilde h_0\right]L^{\theta/\nu}-\frac{B(\alpha)}{\theta/\nu}h^*} . \tag{2.12}$$

Note that from now on, $-\theta/\nu$ always refers to the leading irrelevant exponent for the stable fixed point.

As usual, one expects that exponents are universal. Here universality means that the value of the α-dependent exponents are independent of the underlying lattice (square, triangular, random) or of the details of the probability distribution other than the power-law tail. Amplitudes and values of the flowing parameters are not universal. In particular, in the field theory, the formal expression for $h_0=(-w_0)^{-\alpha}\nu_0$ is complex for w_0 positive although the recursion relations always take h to real values sufficiently near the fixed point. On the other hand, within the nonperturbative nodes-links-blobs approach discussed in Sec. II B, h_0 is real and positive for all initial distributions. Hence, while the field-theoretic approach yields useful formal expressions for t and θ/ν and the correct qualitative behavior for t as a function of

α, it has the unphysical feature that the nonuniversal initial condition Δ is complex for some initial probability distributions. For quantitative comparison with simulation, it is thus preferable to employ the nodes-links-blobs approach developed by Machta, Guyer, and Moore.[10]

B. Nodes-links-blobs analysis

This theory is based on a hierarchial model of the percolation backbone introduced by Given and Mandelbrot[24] and de Arcangelis *et al.*[25] Figure 1 illustrates the rules for the construction of the hierarchial network which serves as a building block for the backbone. For $p=p_c$, the hierarchial construction is continued for N steps until $c^N=L^v$ where $c=2$ is the number of singly connected bonds in one unit of the lattice. On each bond of this network we put a resistor chosen from an initial probability density, $p_o(R)$ satisfying Eq. (1.1). At each stage in the construction the resistance of the network is a random variable governed by a probability distribution, $p_n(R)$. This model incorporates the relevant features of the nodes-links-blobs picture of the percolation backbone.

The primary step in the analysis is the construction of an approximate renormalization group which takes p_n to p_{n+1}. The renormalization-group flows are studied in a two-parameter space of distributions having Laplace transform

$$f(z)=\exp[-(Az)^{\alpha}-Bz]\ , \tag{2.13}$$

where A and B are non-negative. For $A\neq 0$, probability distributions corresponding to Eq. (2.13) are stable distributions[26] with exponent α, which have been shifted by B along the real axis. For $A=0$, Eq. (2.13) corresponds to a δ-function probability density concentrated at B.

The space of distributions defined by Eq. (2.13) is closely related to the space of distributions employed in the field theory and the recursion relations for A and B lead to the same fixed-point structure as found in the field theory. The advantage of using the distributions, Eq. (2.13), is that they are well-defined probability distributions if and only if A and B are non-negative. On the other hand, for the expansion defined in Eq. (2.1), the question of whether f is the Laplace transform of a probability distribution may not be determined by the parameters v and w. For example, if v and w are positive, f is the Laplace transform of a distribution only if the higher-order terms are sufficiently large. We believe that the neglect of these higher-order terms in the field theory leads to the unphysical results—Δ and, hence, t_{eff} complex–for positive w_0.

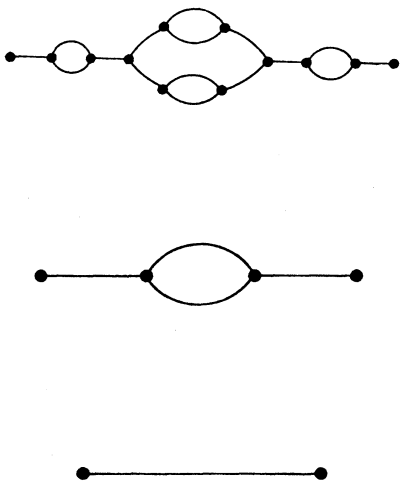

FIG. 1. Hierarchial construction employed to model the percolation backbone.

By comparing the first two terms in Eq. (2.1) and the expansion of Eq. (2.13) we make the identifications $(-w)=B$ and $h=(A/B)^{\alpha}$ between the field-theoretic and hierarchial renormalization group. Defined in terms of A and B, $(-w)$ and h are non-negative so that Δ and t_{eff} are always real. Our assumption is that by keeping more terms in the field theory we would find that the scaling variables corresponding to $(-w_0)$ and h_0 would have the required non-negative property.

Based on the fixed-point values of A and B and the above identification with h we obtain the fixed-point value of h^*

$$h^*=(c^{1/\alpha}-c-a)(c^{1/\alpha}-c)^{\alpha-1}a^{-\alpha}\ , \tag{2.14}$$

where $a=\frac{1}{2}$ and $c=2$. We may also obtain an expression for the leading irrelevant exponent valid in the α-dependent regime, where (2.14) is the stable fixed point, by linearizing the hierarchial recursion relations around this α-dependent fixed point. The result is

$$\theta=\ln\left[\frac{ac^{1/\alpha}+\alpha c^{1/\alpha}(c^{1/\alpha}-c-a)}{ac^{1/\alpha}+\alpha c(c^{1/\alpha}-c-a)}\right]/\ln c \quad \text{for } \alpha<\alpha_c\ . \tag{2.15}$$

For quantitative comparisons with numerical work, we believe that this value of θ is more accurate than the field-theoretic value. Table I shows values of θ/ν for $d=2$ and selected values of α. It is striking that previous numerical simulations disagree with the theory most strongly where θ/ν is smallest.

In order to test the predictions of Eq. (2.8) for the dependence of t_{eff} on the initial distribution it is necessary to vary the initial distribution in a way which changes Δ. The predictions are that t_{eff} approaches the lattice value from above in the α-independent regime ($\alpha>\alpha_c$), but may approach the α dependent value either from above or below. This follows from the fact that h^* negative for $\alpha>\alpha_c$ and positive for $\alpha<\alpha_c$ leading to Δ which is negative definite for $\alpha>\alpha_c$ but may take either sign for $\alpha<\alpha_c$.

The observation that the parameter B in Eq. (2.13) corresponding to a shift leads us to consider a class of initial distributions, $p(R|\alpha,S)$ which are shifted power laws

TABLE I. The ratio of the correction to scaling to the correlation length exponent. For $\alpha<\alpha_c$, θ is obtained from Eq. (2.15), for $\alpha\geq\alpha_c$, θ is obtained from Eq. (2.9). The values, $\nu=\frac{4}{3}$ and $t_0=1.33$ are used where applicable.

α	θ/ν
0.1	5.4
0.2	2.2
0.3	1.2
0.4	0.67
0.5	0.39
0.6	0.20
0.667	0.10
0.7	0.06
0.8	0.03
0.9	0.13
1.0	0.23

$$P(R|\alpha,S)=\alpha(R-S)^{-\alpha-1}\Theta(R-S-1)\ , \tag{2.16}$$

with the shift parameter, $S>-1$ and Θ the unit step function. This class of distributions is contained in the universality class defined by the characteristic exponent α, it is easy to implement numerically, and $S=0$ corresponds to the conventional distribution, Eq. (1.2). The parameter S plays essentially the role of B since both shift the distribution without changing the amplitude of the power-law tail. We can now express Δ in Eq. (2.10) approximately in terms of S and find an S^* for which the leading corrections to scaling vanish. In order to find S^* we expand the Laplace transform of $P(R|\alpha,S)$ to order z

$$\int p(x|\alpha,S)dx\, e^{-zx}=1-z^{\alpha}\Gamma(1-\alpha) -z\left[S-\frac{\alpha}{1-\alpha}\right]+\cdots\ . \tag{2.17}$$

Comparing with Eq. (2.13) we obtain

$$h_0=(A/B)^{\alpha}=\Gamma(1-\alpha)\left[S-\frac{\alpha}{1-\alpha}\right]^{-\alpha}\ . \tag{2.18}$$

For $\alpha>\alpha_c$ the leading finite-size correction vanishes if $\Delta\to\infty$, which occurs when $h_0=0$. On the other hand, for $\alpha<\alpha_c$ the leading finite-size correction vanishes when $\Delta=0$, which occurs when $h_0=h^*$. Equation (2.18) then gives

$$S^*=\begin{cases}[\Gamma(1-\alpha)/h^*]^{1/\alpha}+\dfrac{\alpha}{1-\alpha}, & \alpha<\alpha_c\\ \infty, & \alpha>\alpha_c\ ,\end{cases} \tag{2.19}$$

with the value (2.14) for h^*. For $S>S^*$, $t_{\rm eff}$ approaches its asymptotic value from below and vice versa. According to Eq. (2.19), $S^*>0$ so that, for the conventional distribution ($S=0$), we predict that $t_{\rm eff}>t$, in agreement with previous numerical work. For $\alpha=\frac{1}{2}$, $S^*=2.4$ while for $\alpha=\frac{2}{3}$, $S^*=12.6$.

III. NUMERICAL SIMULATIONS

In Sec. III A we consider the shifted distributions introduced in the previous section to show that, for the lattice sizes used in practice, the effective exponent depends strongly on the shift, S, despite the fact that S is an irrelevant variable. In Sec. III B, we introduce a new parameterless renormalization procedure for the conductivity distribution which shows that, for large enough systems, the exponents do approach the theoretical asymptotic values. At the end of this section, we combine both numerical methods to demonstrate that, in the α-dependent regime, the effective exponent can approach the asymptotic value either from above or below. We conclude by exhibiting semiquantitative agreement between theoretical and simulation values of the correction to scaling exponent θ/ν.

In order to obtain good statistics within a reasonable time, we have carried out computations on small networks though in Sec. III B these are used to construct much larger effective systems. In conventional simulations it is found[11] that effective exponents calculated from systems of sizes 7–10 are identical, within a statistical uncertainty of ±0.04, to the effective exponents obtained from systems of size 20–23. Because of the small value of θ, the effective exponent changes very little between "small" systems of size 5–10 and systems of size 20 or even 100, the latter being of the order of the largest sizes studied by state of the art methods. Thus, to go to much larger systems and observe the approach to the asymptotic exponent, one must resort to an approximation such as the renormalization procedure described in Sec. III B.

A. Shifted distributions

The shift parameter S introduced in Eq. (2.16) enters the renormalization-group equations only through the initial value h_0 [see Eq. (2.18)], and does not influence the value of the asymptotic conductivity exponent. In other words, all distributions which differ only by their value of S are on the same critical manifold and all flow to the same fixed point under renormalization. Nevertheless, h flows very slowly towards the fixed point so that the irrelevant parameter S has a large effect on the effective value of the conductivity exponent obtained from small systems. This is illustrated in Fig. 2, for the case $\alpha=\frac{2}{3}$, by a plot of the value of effective exponent $t_{\rm eff}/\nu$ versus S obtained for small system sizes. The noteworthy features of this figure are that $t_{\rm eff}/\nu$ can be larger or smaller than the asymptotic value of $\frac{9}{8}$ and the effective exponent equals the asymptotic result at a value of S which is close to the nodes-link-blobs prediction $S^*=12.6$. Similar results hold for the case $\alpha=\frac{1}{2}$, where the observed value of S^* is approximately 2, while the nodes-links-blobs prediction is $S^*=2.4$.

B. Parameterless renormalization of the conductivity distribution

In the standard percolation problem, the geometrical exponents, and even the conductivity exponent, are quite close to their asymptotic values for systems as small as

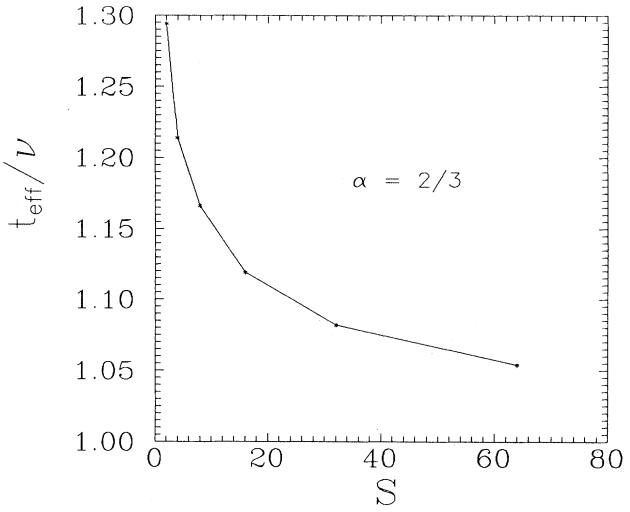

FIG. 2. Effective conductivity exponent, $t_{\rm eff}/\nu$, for shifted distributions defined in Eq. (2.16) as a function of the shift parameter S for $\alpha=\frac{2}{3}$. For each value of S, the exponent is obtained from log-log plots of the average conductivity as a function of L. The asymptotic value of the exponent is 1.13. The average, for each value of L, was over 2×10^5 conducting samples of $L\times L$ lattice of size $L=5, 6, 7$.

$L\approx10$. Hence, replacing every bond of a 10×10 system by a realization of another 10×10 percolating network yields a system which behaves very much like a 100×100 network. We use this property in a numerical renormalization procedure for continuum percolation which permits us to study, in an approximate way, systems much larger than those accessible by direct simulation. The following algorithm is applied iteratively to N samples of bond-diluted lattices of size L at the bulk percolation threshold ("size L" refers to an $L\times L$ square lattice and $p_c=0.5$).

(1) The initial set of conducting bonds ($n=0$) are chosen from the cumulative probability distribution defined in Eq. (1.2). At the nth iteration ($n>0$), the conductivities of the conducting bonds are chosen from the cumulative probability distribution obtained at the $(n-1)$th iteration.

(2) The conductivity of each of the N resulting $L\times L$ networks is computed using a method described in Ref. 27.

(3) The conductivities of these N percolating networks are then used to define the nth *cumulative* probability distribution. The cumulative probability distribution is found[28] by sorting, in increasing order, the conductivities obtained by step (2). The cumulative probability distribution is zero for all conductivities less than the smallest one, and unity for all conductivities greater than the largest one. Between these limits the cumulative probability is obtained by incrementing by $1/N$ at each successive conductivity, starting from the smallest.

Steps (1)–(3) are iterated n times in order to simulate a system whose effective size, $L_{\rm eff}$ is given by $L_{\rm eff}=L^{n+1}$. For a given size, $L_{\rm eff}=L^{n+1}$ of interest, the corresponding conductivity exponent is obtained by computing the conductivity of lattices of sizes L, $L+1$, $L+2$ whose bond conductivities are all drawn from the probability distribution used at the beginning of the nth iteration. This is effectively like computing the conductivities for sizes L^nL, $L^n(L+1)$, and $L^n(L+2)$ and determining the exponent from a log-log plot of conductivity versus size. Note that to obtain an exponent for systems of size $L_{\rm eff}$, the results for systems of size $L_{\rm eff}/L$ are not used: the procedure is started anew to avoid statistical dependencies. We are effectively doing a parameterless rescaling of the probability distribution of the conductivities. The preceding procedure may also be viewed as a way to generate distributions which are closer to the fixed-point distribution and thus have smaller corrections to scaling.

The results are illustrated in Fig. 3 for $\alpha=\frac{2}{3}$, and in Fig. 4 for $\alpha=0.9$ and $\frac{1}{2}$. Indeed, for $\alpha=\frac{2}{3}$ and $\alpha=\frac{1}{2}$, the effective exponent decreases towards its theoretical value $t_{\rm eff}/\nu=1/(\alpha\nu)$ as the effective size, $L_{\rm eff}$, increases. Consider in particular, Fig. 3 for $\alpha=\frac{2}{3}$. $t_{\rm eff}/\nu$ reaches a plateau somewhat above its theoretical value $\frac{9}{8}$, before plunging towards the lattice value $t_{\rm eff}/\nu\approx0.98$. The latter behavior is easy to understand qualitatively as follows. Since the number of initial samples, N, is finite, the first renormalized probability distribution obtained from these N sample lattices has a cutoff in the tail instead of a tail that extends all the way to $\sigma=0$. At each stage, the tail of the distribution is cut off at larger and larger conductivities compared with the typical conductivity.

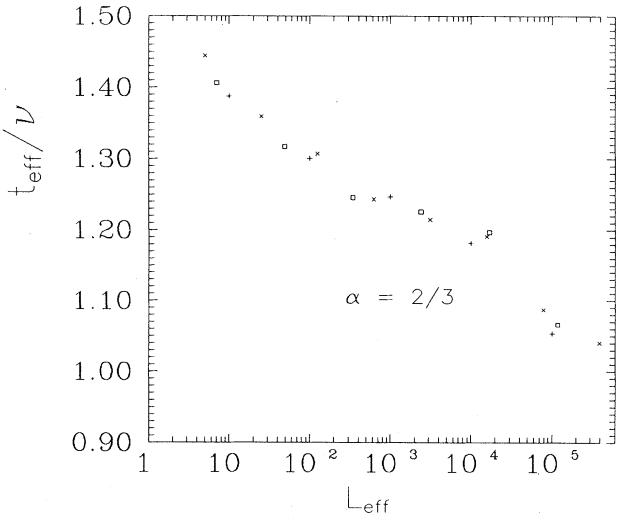

FIG. 3. Conductivity exponent, $t_{\rm eff}/\nu$, as a function of the effective system size, $L_{\rm eff}$, on a logarithmic scale, for $\alpha=\frac{2}{3}$. ×'s correspond to renormalization of systems of size 5^{n+1}, squares to systems of size 7^{n+1}, and crosses to systems of size 10^{n+1}. 50 000 samples are used at every level of rescaling, and the samples used for any point on this graph are statistically independent from the samples used for any other point. For systems of size 7^{n+1}, 10^{n+1}, the effective exponents are averaged over three complete rescaling procedures, while the average was over five rescaling procedures for systems of size 5^{n+1}.

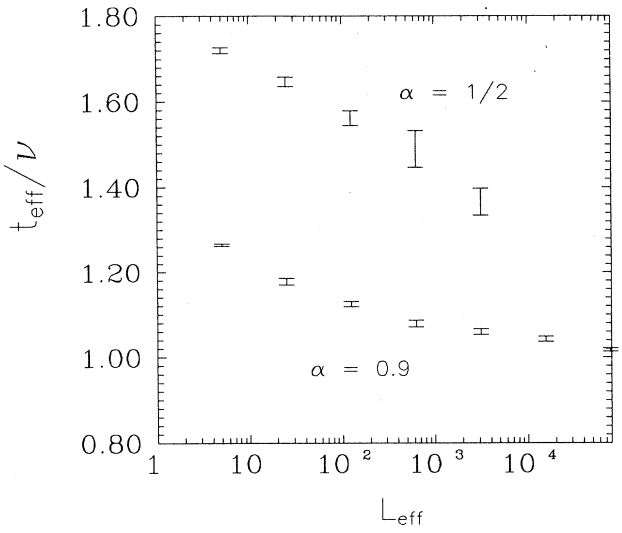

FIG. 4. Conductivity exponent t_{eff}/ν as a function of the effective system size L_{eff}, on a logarithmic scale, for $\alpha=0.9$ (lower set of points) and $\alpha=\frac{1}{2}$ (upper set of points). All the points correspond to renormalization of systems of size 5^{n+1}. 50 000 samples are used at every level of rescaling, and the samples used for any point on this graph are statistically independent from the samples used for any other point. The error bars are obtained by repeating the whole calculation of the effective exponents three times for $\alpha=0.9$, and seven times for $\alpha=\frac{1}{2}$.

When the smallest conductivity in the distribution is of the same order as the typical conductivity of the network, the effect of the tail of the distribution is lost and further iteration of the distribution causes the effective exponent to approach the universal value.

To what extent does the system obtained by the above numerical procedure faithfully reproduce the effective exponents for a system of size $L_{\text{eff}}=L_{n+1}$? We can give the following qualitative arguments that the approximation is a good one for L of order 10. For lattice percolation the geometrical exponents and even the conductivity exponent are quite close to their asymptotic values for systems as small as $L\approx 10$. Thus, we believe that the topological features of a network of size 10 are sufficient to yield good values of the conductivity exponent so long as the distribution of resistances is near its fixed point. Iteration of the numerical procedure brings the distribution close to the fixed point in a realistic way.

The following feature of the results shown in Fig. 3 also gives us confidence in the validity of the approach: For different values of L, say $L_1=5$ (crosses) and $L_2=7$ (squares), the effective exponents for sufficiently large system sizes are identical when $L_1^{n_1+1}\approx L_2^{n_2+1}$. See, for example, the cases $L=5$, $n=5$ and $L=7$, $n=4$, where $L_{\text{eff}}\approx 1.6\times 10^4$. Note also how the value of the effective exponent obtained for $n=5$ iterations and $L=7$ ($L_{\text{eff}}=117\,649$) is quite different from the exponent for the same number of iterations, $n=5$, but for a different value $L=5$ ($L_{\text{eff}}=15\,625$). In the former case the exponent has started to crossover to the lattice value while in the latter case it is still in the vicinity of the continuum value. In general, the similarity of the results for the three different sizes, $L=5$, 7, 10, lead us to believe that t_{eff} is a function of the effective size, L_{eff} but not of L or n independently.

In the case $\alpha=0.9$, illustrated in Fig. 4, the effective exponent decreases monotonously towards the universal lattice value. One could argue that the same cutoff effect just discussed for $\alpha=\frac{2}{3}$ will lead to the lattice value for the exponent anyway, but we believe that at least the initial decrease is independent of that cutoff. More troublesome is the absence, in the case $\alpha=\frac{1}{2}$, of a plateau around the theoretical value $t/\nu=1.5$. In this case, we think this may come from the fact that the correction to scaling exponent θ/ν is much larger than in the $\alpha=\frac{2}{3}$ case (four times larger according to Table I). This may also reflect itself in the rate of disappearance of the tail. We did not, however, find a criterion which would tell us unambiguously when we can neglect the effect of the cutoff in the tail.

The two numerical methods described above may be combined to add credence to the overall correctness of the picture. We repeat the renormalization procedure just described, except that we choose a shifted initial distribution as defined in Eq. (2.16). In Fig. 5 we show t_{eff} as a function of L_{eff} for $S=40$ and $\alpha=\frac{2}{3}$. In accord with the theory, for this value of S the effective exponent starts

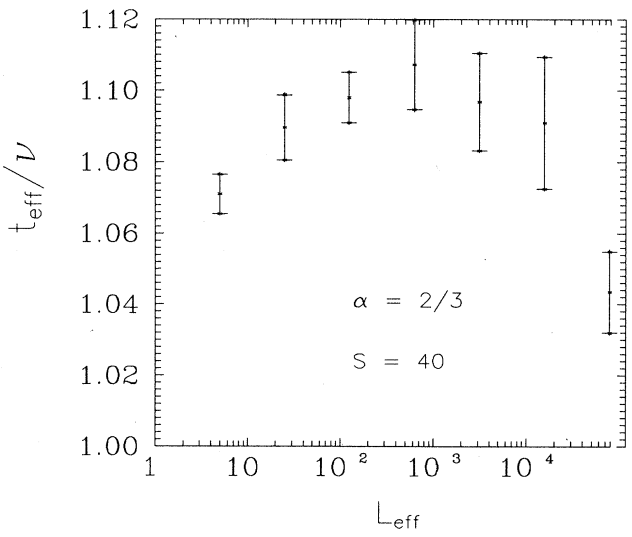

FIG. 5. Conductivity exponent, t_{eff}/ν, for the shifted distribution of Eq. (2.16) with $S=40$, as a function of the effective system size L_{eff}, on a logarithmic scale, for $\alpha=\frac{2}{3}$. All the points correspond to renormalization of systems of size 5^{n+1}. 50 000 samples are used at every level of rescaling, and the samples used for any point on this graph are statistically independent from the samples used for any other point. The error bars are obtained by repeating the whole calculation of the effective exponents six times.

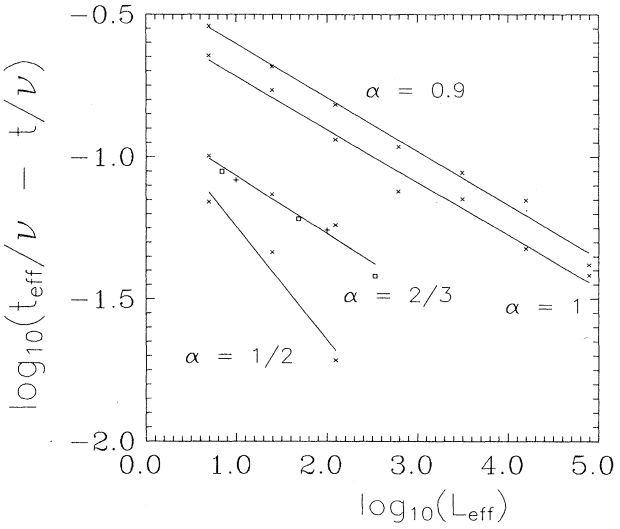

FIG. 6. Plots yielded the correction to scaling exponents, θ/ν, for $\alpha=1$, 0.9, $\frac{2}{3}$, and $\frac{1}{2}$. Since the first-order expansion in $L^{-\theta/\nu}$ of either Eq. (2.8) or (2.12) suffices to describe the results, an estimate of θ/ν is obtained from the slope of the plot $\log(t_{\rm eff}/\nu-\tau/\nu)$ vs $\log(L_{\rm eff})$, where t is given by Eqs. (1.4) and (1.6) and $t_{\rm eff}/\nu$ is obtained from the renormalization procedure described in Sec. III B. The same data as in Figs. 3 and 4 (plus analogous data obtained for the case $\alpha=1$) are used. ×'s correspond to renormalization of system of size 5^{n+1}, squares to systems of size 7^{n+1}, and crosses to systems of size 10^{n+1}. The straight lines are least-squares fits used to obtain an estimate of the slope. In the case $\alpha=\frac{2}{3}$ and $\frac{1}{2}$, only the data for $t_{\rm eff}>t$ is kept because for $t_{\rm eff}<t$ the renormalization procedure is unstable as explained in the text. For clarity of display, the data for $\alpha=\frac{2}{3}$ and $\alpha=\frac{1}{2}$ are shifted down by -0.5. The logarithms are base 10.

below the asymptotic value, $\frac{9}{8}$, and rises toward it. The effective exponent eventually plunges toward the lattice value because of the tail-cutoff effect.

To conclude, note that fitting the data to Eqs. (2.8) or (2.12), we may obtain an estimate of the correction to scaling exponent, θ/ν. We observed that, in practice, the first-order expansion in $L^{-\theta/\nu}$ of these expressions gives a reasonable account of the data. This kind of expansion is also done in Eq. (7) of Ref. 20, for example. For $\alpha=1$, 0.9, $\frac{2}{3}$, and $\frac{1}{2}$, we obtain, from Fig. 6, the respective values 0.19, 0.19, 0.2, and 0.4, which should be compared to the corresponding values from Table I, namely, 0.23, 0.13, 0.1, and 0.4. The agreement is not very good for small values of θ/ν, but this is expected given the statistical errors and the smallness of the exponent. Furthermore, both the node-links-blobs model and the numerical rescaling procedure are approximations so that quantitative agreement cannot be expected. Nonetheless, these numbers suffice to show the qualitative trends and the smallness of θ/ν in regions where past numerical simulations have conflicted with theory.

IV. CONCLUSION

We have shown that in the continuum percolation problem there is a very small correction to the scaling exponent, θ (see Table I and Fig. 6). That exponent describes the rate of convergence of the dimensionless variable h, associated with the shape of the probability distribution, towards its fixed-point value. The exponent θ becomes arbitrarily small as α approaches the point, α_c, where the lattice and continuum fixed points exchange stability. In finite-size calculations, using the conventional power-law distribution, this leads to effective exponents which differs markedly from their asymptotic values even for extremely large system sizes. In Sec. II we estimated the effective conductivity exponent using both a field theory[11,13,14] and a nodes-links-blobs[10] approach. For quantitative estimates at small values of α, one must rely on the latter approach. The present study strongly suggests that finite-size effects have led to the disagreement between previous simulations and theory in the vicinity of $\alpha=\alpha_c$ where the fixed points exchange stability. Though this disagreement is at most of order 30%, it could have suggested qualitative errors in theory.

We have introduced two types of numerical simulations which support the correction to scaling theory. In Sec. III A we used shifted initial distributions which all are in the same universality class but differ by the initial value of the irrelevant shift parameter. The fact that the effective exponent depends on the shift parameter demonstrates that the systems sizes which are used in practice and are adequate for obtaining lattice exponents are not large enough for studying broad distributions.

The second type of numerical approach also corresponds in a sense to varying the initial distribution. More specifically, we simulated N samples of the percolating resistor network and used the resistances of this ensemble to define a renormalized probability. This parameterless renormalization of the conductance distribution, displayed in Figs. 3 and 4, shows that the asymptotic value of the exponent is reached for unusually large system sizes. The eventual fall of the effective exponents toward their lattice value comes from the finite number of samples which leads to a cutoff in the tail of the renormalized distribution.

Finally, we combined both numerical methods. By varying the initial distribution and then going to very large systems using the numerical renormalization procedure we demonstrated, see Figs. 3 and 5, that the effective exponent can approach the asymptotic value either from above or below for $\alpha<\alpha_c$. This approach should be useful in studying the continuum corrections to the noise exponent[6] since the conductivity exponent also comes indirectly in the result.[29,30] The general ideas of the numerical techniques introduced here could prove useful for other disordered systems.

We should caution that the convergence of effective exponents to their asymptotic value is so slow that even physical experiments on disordered systems with a broad distribution characterizing the disorder must be interpreted with care. The finite-size effects encountered in

numerical simulations translate into an extremely narrow critical region around p_c in physical experiments.

ACKNOWLEDGMENTS

We are especially indebted to Pierre Breton and Marc-André Lemieux for computer programming, to Kevin Hood for help with the DEFINICON DSI-020 board, to T. Lubensky for variable discussions, and to V. Privman for pointing out a reference. One of us (J.M.) is supported by the National Science Foundation (NSF) under Grant No. DMR-87-02705. One of us (A.-M.S.T.) would like to acknowledge the hospitality of Cornell University, where this work was begun. Support there was provided by the NSF under Grant No. DMR-85-166-16 administered by the Cornell University Materials Science Center. Early calculations were performed—with thanks to M. Nelkin—through the Cornell Theory Center, which is supported in part by the National Science Foundation, New York State, and the IBM Corporation. One of us (A.-M.S.T.) is supported by the Natural Sciences and Engineering Research Council of Canada, by the Fonds pour la Formation des Chercheurs et l'Aide á Recherche (Québec), and by the Steacie Foundation.

[1]B. I. Haplerin, S. Feng, and P. N. Sen, Phys. Rev. Lett. **54**, 2391 (1985); S. Feng, B. I. Halperin, and P. N. Sen, Phys. Rev. B **35**, 197 (1987).

[2]J. Machta and S. M. Moore, Phys. Rev. A **32**, 3164 (1985).

[3]M. A. Dubson and J. C. Garland, Phys. Rev. B **32**, 7621 (1985); M. Octavio, G. Gutierrez, and J. Aponte, *ibid.* **36**, 2461 (1987).

[4]L. Benguigui, Phys. Rev. B **34**, 8176 (1986).

[5]C. J. Lobb and M. G. Forrester, Phys. Rev. B **35**, 1899 (1987); L. N. Smith, C. J. Lobb, *ibid.* **20**, 3653 (1979).

[6]For a review, see A.-M.S. Tremblay and B. Fourcade, Physica A **157**, 89 (1989).

[7]P. M. Kogut and J. P. Straley, J. Phys. C **12**, 1251 (1979).

[8]A. Ben-Mizrahi and D. J. Bergman, J. Phys. C **14**, 909 (1981).

[9]J. P. Straley, J. Phys. C **15**, 2333 (1982); **15**, 2343 (1982).

[10]J. Machta, R. A. Guyer, and S. M. Moore, Phys. Rev. B **33**, 4818 (1986).

[11]T. C. Lubensky and A.-M. S. Tremblay, Phys. Rev. B **34**, 3408 (1986).

[12]P. LeDoussal, Phys. Rev. B **39**, 881 (1989).

[13]J. Machta, Phys. Rev. B **37**, 7892 (1988).

[14]T. C. Lubensky and A.-M. S. Tremblay, Phys. Rev. B **37**, 7894 (1988).

[15]P. N. Sen, J. N. Roberts, and B. I. Halperin, Phys. Rev. B **32**, 3306 (1985).

[16]A. Bunde, H. Harder, and S. Havlin, Phys. Rev. B **34**, 3540 (1986).

[17]A. L. R. Bug, G. S. Grest, M. H. Cohen, and I. Webman, Phys. Rev. B **36**, 3675 (1987).

[18]M. Murat, S. Marianer, and D. J. Bergman, J. Phys. A **19**, L275 (1986).

[19]X. C. Zeng, D. J. Bergman, and D. Stroud, J. Phys. A **21**, L949 (1988).

[20]V. Privman and M. E. Fisher, J. Phys. A **16**, L295 (1983). See also J. Adler, M. Moshe, and V. Privman, in *Percolation, Structures and Processes,* edited by G. Deutscher, R. Zallen, and J. Adler (Annals of the Israel Physical Society, Israel, 1983), Vol. 5, for a review of earlier work.

[21]J. R. Banavar, A. J. Bray, and S. Feng, Phys. Rev. Lett. **58**, 1463 (1987).

[22]"α" as used here is equal to one minus "α" of Refs. 8, 15–17, 19, and (1a) of Ref. 11.

[23]J. G. Zabolitzky, Phys. Rev. B **30**, 4077 (1984); H. J. Herrmann, B. Derrida, and J. Vannimenus, *ibid.* **30**, 4080 (1984); D. C. Hong, S. Havlin, H. J. Herrmann, and H. E. Stanley, *ibid.* **30**, 4083 (1984); R. Rammal, J. C. Angles d'Auriac, and A. Benoit, *ibid.* **30**, 4087 (1984); C. J. Lobb and D. J. Frank, *ibid.* **30**, 4090 (1984).

[24]B. B. Mandelbrot and J. A. Given, Phys. Rev. Lett. **52**, 1853 (1984).

[25]L. de Arcangelis, S. Redner, and A. Coniglio, Phys. Rev. B **31**, 4725 (1985).

[26]See, W. Feller, *An Introduction to Probability Theory and Its Applications,* 2nd ed. (Wiley, New York, 1971), Vol. 2, for a detailed discussion of the properties of Laplace transforms of distributions and the theory of stable distributions.

[27]M.-A. Lemieux and A.-M.S. Tremblay, Phys. Rev. B **36**, 1463 (1987).

[28]W. H. Press, B. P. Flannery, A. S. Teukolsky, and W. T. Vetterling, *Numerical Recipes* (Cambridge University, London, 1986).

[29]G. A. Garfunkel and M. B. Weissman, Phys. Rev. Lett. **55**, 296 (1985).

[30]A.-M. S. Tremblay, S. Feng, and P. Breton, Phys. Rev. B **33**, 2077 (1986).